Received: 20 January 2017 | Revised: 5 June 2017 | Accepted: 19 June 2017

DOI: 10.1002/prot.25340

RESEARCH ARTICLE

WILEY

Exploration of conformational changes in lactose permease upon sugar binding and proton transfer through coarse-grained simulations

Yead Jewel | Prashanta Dutta | Jin Liu

School of Mechanical and Materials Engineering, Washington State University, Pullman, Washington 99164

Correspondence
Jin Liu, School of Mechanical and Materials Engineering, Washington State University, Pullman, WA 99164, USA.
Email: jin.liu2@wsu.edu

Funding information
US National Science Foundation, Grant/Award Number: CBET-1604211; Extreme Science and Engineering Discovery Environment (XSEDE), Grant/Award Number: MCB170012

Abstract

Escherichia coli lactose permease (LacY) actively transports lactose and other galactosides across cell membranes through lactose/H^+ symport process. Lactose/H^+ symport is a highly complex process that involves sugar translocation, H^+ transfer, and large-scale protein conformational changes. The complete picture of lactose/H^+ symport is largely unclear due to the complexity and multiscale nature of the process. In this work, we develop the force field for sugar molecules compatible with PACE, a hybrid and coarse-grained force field that couples the united-atom protein models with the coarse-grained MARTINI water/lipid. After validation, we implement the new force field to investigate the binding of a β-D-galactopyranosyl-1-thio-β-D-galactopyranoside (TDG) molecule to a wild-type LacY. Results show that the local interactions between TDG and LacY at the binding pocket are consistent with the X-ray experiment. Transitions from inward-facing to outward-facing conformations upon TDG binding and protonation of Glu269 have been achieved from ∼5.5 μs simulations. Both the opening of the periplasmic side and closure of the cytoplasmic side of LacY are consistent with double electron–electron resonance and thiol cross-linking experiments. Our analysis suggests that the conformational changes of LacY are a cumulative consequence of interdomain H-bonds breaking at the periplasmic side, interdomain salt-bridge formation at the cytoplasmic side, and the TDG orientational changes during the transition.

KEYWORDS
hybrid force field, H-bonding, lactose/H+ symport, LacY, salt-bridges

1 | INTRODUCTION

Transmembrane transporter proteins actively control the traffic of specific molecules across the membranes that surround all cells and organelles. The major facilitator superfamily (MFS) is an important class of transporter proteins that can be found in nearly all life forms.[1] The *Escherichia coli* lactose permease (LacY) is a primary member of MFS and plays essential roles during transport of galactosides across cell membranes.[2,3] As illustrated in Figure 1, LacY is a complex protein composed of 12 transmembrane helices, which are grouped into two pseudosymmetric domains (N-terminal and C-terminal). LacY utilizes a proton gradient to actively drive the passage of galactosides through the membrane against the sugar concentration gradient. The coupled transport of galactoside and proton (lactose/H^+ symport) by LacY has been extensively studied and become the prototype for studying MFS transport mechanisms and applications.[4–6] The molecular transport mechanism of lactose/H^+ symport has been investigated in many biochemical and biophysical experiments,[7–10] based on which a schematic depicting the whole process has been proposed by Guan and Kaback[2] as shown in Figure 1. The complete cycle of lactose/H^+ symport can be decomposed into six steps: (1) LacY is open to the periplasmic side and then the residue Glu269 is protonated; (2) a sugar molecule binds to LacY from periplasmic side; (3) LacY undergoes a dramatic structural reorganization and changes from outward-facing to inward-facing conformation, this occurs simultaneously with H^+ transfer to Glu325; (4) the sugar molecule escapes from LacY and moves to cytoplasmic side; (5) the H^+ is released from Glu325 to cytoplasm; (6) LacY undergoes a series of conformational changes and returns back to the outward-facing state. According to this schematic, the entire process of lactose/H^+ symport can be divided into proton-dependent process with the

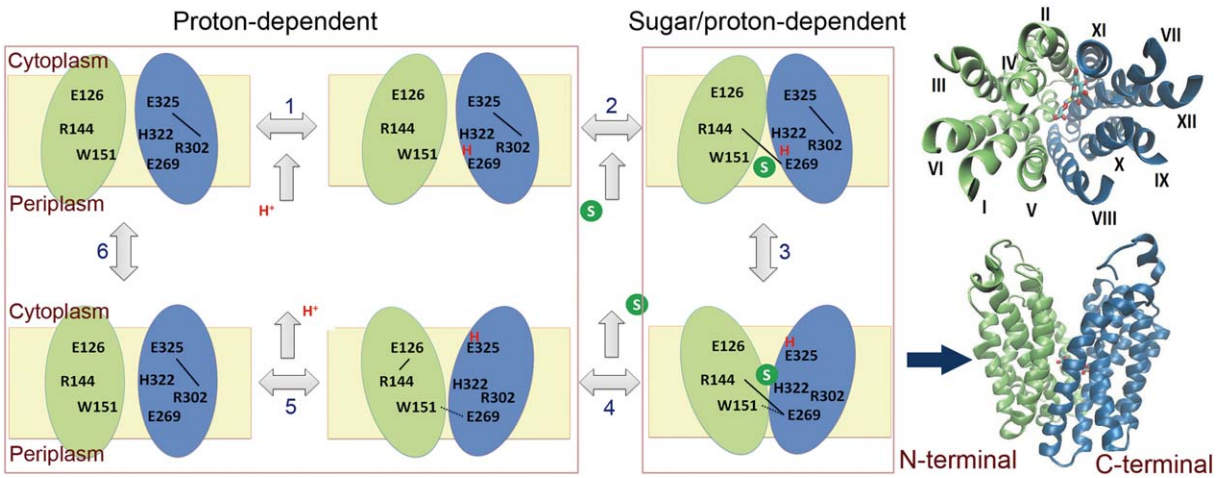

FIGURE 1 Schematic representation of the possible cycle of lactose/H^+ symport and LacY conformational changes according to the work of Guan and Kaback.[2] The important residues are labeled and the important salt-bridges (solid lines) and H-bonds (dashed lines) are indicated in the figure. Right figures (both top-view with labeled helices and side-view) show the new cartoon representation (green for N-terminal and blue for C-terminal domains) of crystal structure (inward-facing) of LacY. [Color figure can be viewed at wileyonlinelibrary.com]

absence of sugar and sugar/H^+-dependent process which involves both the translocation of sugar and H^+ transfer as shown in Figure 1.

The lactose/H^+ symport is a highly complex process that is dictated by collective and cooperative interplay of several dynamic and multiscale events, such as molecular scale sugar translocation and H^+ transfer, and global protein conformational transitions between inward-facing and outward-facing states. Each of these events is a consequence of numerous dynamic molecular interactions involving salt-bridges/H-bonds formations/breakages among protein side chains. Early crystal structures of LacY captured through X-ray experiments are dominant in inward-facing conformations.[11–13] Later, a stable outward-facing mutant was constructed with Trp replacements for two periplasmic Gly residues.[14] An occluded structure of the double-Trp mutant with narrowly opened periplasmic side and tightly sealed cytoplasmic side was determined.[15] Most recently, the crystal structure of a double-Trp mutant with outward-facing conformation was determined in a LacY-nanobody complex.[16] The single-domain camelid nanobodies have been developed to stabilize the outward-facing state. Large amount of experiments—including double electron–electron resonance (DEER),[17] single-molecule fluorescence resonance energy transfer (FRET),[18] site-directed alkylation,[19–22] and site-directed cross-linking[23]—strongly support the alternating access mechanism,[24] in which the LacY should undergo transitions between inward-facing and outward-facing conformations during lactose/H^+ symport. However, the molecular mechanisms dictating the conformational transitions are largely unclear due to the complexity and multiscale nature of the process.

Molecular dynamics (MD) simulations[25–29] have also been employed to investigate the sugar binding/transport processes involved in lactose/H^+ symport and elucidate the transport mechanism. For instance, Yin et al.[25] studied the effects of protonation states of Glu325 and Glu269 on the structural changes of a sugar-bounded LacY in ~10 ns simulations. Holyoake and Sansom[26] explored the effects of substrate binding on LacY conformations over ~50 ns simulations and observed some degree of domain closure. Klauda and Brooks[27] probed the protein–sugar interactions, binding structures, and protein motions in response to substrate binding to both mutant and wild-type LacY in ~20–25 ns simulations. Later, Jensen et al.[28] explored the molecular and energetic details during sugar conduction across LacY using steered molecular dynamics. Nevertheless, those simulations have either focused on sugar binding process with small conformational changes of LacY[25–27] or sugar transport across LacY with the aid from some external means.[28] The outward-facing conformation of LacY has been generated by Radestock and Forrest[30] through swapping the conformations of the repeat units in each half of the structure, the structured has been found consistent with previous experiments. Moreover, Klauda et al.[29,31] have probed the periplasmic-open state of LacY using a two-step hybrid implicit–explicit molecular simulation approach, in which the conformational transition to periplasmic-open state was explored by self-guided Langevin dynamics simulations in implicit membrane environment.

In this work, we investigate the sugar binding and the coupled LacY conformational changes through coarse-grained (CG) molecular simulations using the hybrid PACE force field. The PACE force field was originally developed by Han et al.[32–37] In PACE, a united-atom-based protein model is coupled with the MARTINI[38,39] water/lipid environment. Through coarse-graining of the environmental molecules (water and lipid), the molecular simulation time can be significantly extended while the molecular details of the protein are still retained. The PACE force field has been employed to study the folding and unfolding events in several peptides[35] and small proteins[36] in microsecond simulations. We have recently implemented the PACE force field to investigate the proton-dependent dynamics and conformational changes of LacY without sugar molecule,[40] and we were able to observe the transition from inward-facing to outward-facing conformations of LacY in microsecond molecular simulations. Here we

first extend the PACE force field to include sugar interactions, and then implement the new force field to study lactose/H^+ symport with focus on the important roles of sugar molecule during sugar binding and the associated large-scale conformational changes of LacY.

2 | MATERIALS AND METHODS

2.1 | PACE protein model

PACE is a hybrid force field developed by Han et al.[32–37] with a united-atom-based model (each heavy atom represents one site) for proteins coupled with the coarse-grained MARTINI[38,39] water and lipid model (four heavy atoms represent one site). In protein models, each heavy atom with the attached hydrogen atoms is generally modeled with one site, but the hydrogens on backbone and side-chain amide groups are also explicitly expressed for better accounting of H-bonding. Both bonded and nonbonded interactions are included in PACE and the total energy of the system can be expressed as follows:

$$E = E_{\text{bond}} + E_{\text{angle}} + E_{\text{dihedral}} + E_{\text{improper}} + E_{\varphi,\psi,\chi_1} + E_{\text{W-W}} + E_{\text{W-P}} + E_{\text{vdW}} + E_{\text{polar}} \quad (1)$$

The first four terms account for bonded interaction mediated by covalent bonds and the last four terms account for the nonbonded interactions including water–water interactions ($E_{\text{W-W}}$), water–protein interactions ($E_{\text{W-P}}$), interactions between nonpolar protein sites (E_{vdW}), and interactions between polar interactions (E_{polar}). E_{φ,ψ,χ_1} is for the interactions involved with rotamers of the backbone (ϕ and ψ) and the side chains (χ_1). The Lennard–Jones (LJ) potential is used for nonbonded interactions:

$$E_{ij} = \sum_{i \neq j} 4\varepsilon_{ij}\left(\frac{\delta_{ij}^{12}}{r_{ij}^{12}} - \frac{\delta_{ij}^{6}}{r_{ij}^{6}}\right). \quad (2)$$

Here, ε_{ij} represents the interparticle binding energy and δ_{ij}, the van der Waals radius. r_{ij} is the distance between particles i and j. For bonded interactions in Equation 1, the equilibrium bond length and angle values were taken from the optimized geometries by quantum mechanics (QM) calculation. The dihedral parameters were obtained by fitting QM dihedral potential profiles of small molecules. Improper terms were used to maintain the planarity or chirality of groups. The interaction parameters for E_{φ,ψ,χ_1} were obtained through iterative equilibrium simulations against side-chain rotamer distributions and rotamer-dependent backbone conformations from a coil library. The parameters for water–protein interactions in Equation 2 were optimized from fitting hydration free energies of 35 small organic molecules. E_{vdW} parameters were obtained on the basis of densities of liquid states and free energies of evaporation of 8 organic compounds. The polar and charged sites interactions were optimized by fitting the PMFs from all-atom simulations with the OPLS-AA/L[41] force field in explicit water. Details on the modeling development and parameter optimization can be found in Refs. 34,36.

2.2 | The sugar model

In this work, we have extended the original PACE force field to include sugar molecules. We follow the same philosophy as the PACE protein for sugar models. The hydrogen and the attached heavy atom are combined to form one site. The bonded interactions parameters were obtained using the simplified Boltzmann Inversion method.[42] We have developed the sugar–water interactions from the hydration free energy (HFE) calculations. The interactions from the hydroxyl groups on sugar molecules with water molecules represent the dominant interaction; therefore, in our sugar model, we defined a new type of particle representing the hydroxyl group and adjusted the new hydroxyl–water interaction parameters ($\varepsilon_{\text{OH-W}}$ and $\delta_{\text{OH-W}}$ in Equation 2) to match the all-atom result of HFE for β-D-glucose (17.6 ± 0.3 kcal/mol). The interaction parameters for the other atoms on sugar molecule were less important and taken from the original PACE. We have performed our simulations (both coarse-grained and all-atom) in a water box of 48×48×48Å^3, a β-D-glucose molecule was originally placed at the center of the box and then the molecule was pulled out from the water. The potential of mean force (PMF) of the β-D-glucose was calculated and then the HFE was determined. The hydroxyl–water interaction parameters were then adjusted such that the calculated HFE (17.3 ± 0.4 kcal/mol) agreed with the all-atom result. Finally, the parameters were determined as: $\varepsilon_{\text{OH-W}} = 0.78$ kcal/mol and $\delta_{\text{OH-W}} = 3.4$ Å. The interaction is much weaker than the original hydroxyl–water interaction from PACE (3.35 kcal/mol and 2.8 Å respectively). This is due to the fact that the coarse-graining of the water molecules could lead to considerable loss of configurational entropy, missing of the important hydrogen bonding with the water, and the lacking of electrostatic solvation. To confirm our force field, we have also conducted the HFE calculation using free energy perturbation (FEP) approach[43] and the HFEs are 17.0 ± 0.3 kcal/mol for all-atom and 16.4 ± 0.5 kcal/mol for coarse-grained force field. We further confirmed the sugar–water force field through HFE calculation for a β-D-galactopyranosyl-1-thio-β-D-galactopyranoside (TDG) molecule (27.1 ± 0.4 kcal/mol for all-atom and 28.0 ± 0.5 kcal/mol for coarse-grained force field). For the nonbonded interactions with the protein residues (mainly the interactions from the hydroxyl group on sugar molecules with protein residues), we have followed the procedures described in Ref. 36 to adjust the interaction parameters (ε and σ in Equation 2) for the CG sugar model, so that the PMFs from CG force field match with the results from all-atom model. We have performed NPT (T = 300 K and P = 1 atm) simulations in a periodic box of 30×30×30 Å^3 for both CG and all-atom simulations and the PMF profiles were obtained using adaptive biasing force (ABF) method.[44] The final interaction parameters after adjustment were summarized and provided in Supporting Information, Table S1.

The new sugar force field was implemented with PACE to study lactose/H^+ symport. All simulations were performed using the modified version of NAMD 2.10.[45] The original PACE force field were adopted for protein, lipid, water, and ion molecules. The initial configurations were constructed using CHARMM-GUI[46–49] and VMD.[50] Figure 2 illustrates our simulation system. As shown, our system

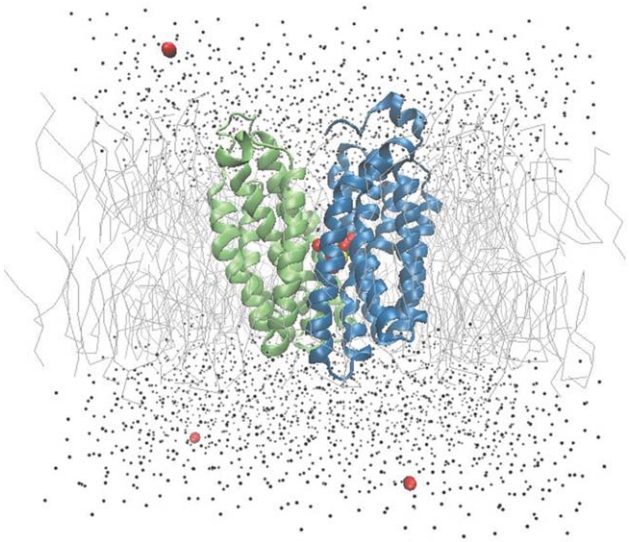

FIGURE 2 The illustration of the simulation box with wild-type LacY (PDB ID: 2V8N) (new cartoon representation with green and blue colors for N-terminal and C-terminal domains) with bound TDG sugar embedded in a POPE (line representation) lipid bilayer. Water and chloride molecules are represented by black and red spheres, respectively. [Color figure can be viewed at wileyonlinelibrary.com]

contains 273 lipids after removal of the lipids overlapping with the protein and ~4200 MARTINI water molecules. To neutralize the system, several chloride ions were added into the system depending on the protonation states. The total system contained ~11,500 atoms with dimensions of ~112 × 112 × 96 Å^3. The lipid bilayer systems were equilibrated using the standard six-step equilibration process[46–49] of gradually turning off the constraints over 280 ps at a temperature of 300 K. In production simulations, periodic boundary conditions were applied in all three directions. The van der Waals interactions were calculated using LJ potential with a cutoff of 12 Å. Production simulations were carried out for ~5.5 μs using NPT ($T = 300$ K and $P = 1$ atm) ensembles. The simulation time-step is set to 4 fs. The time-step is close to the all-atom simulations but the number of atoms is significantly reduced because of the coarse-grained MARTINI water and lipids. VMD has been used for analysis of atomic distances, salt-bridges, H-bonds, and taking snap shots. Pore radius analysis was carried out using HOLE[51] program based on 100-ns blocks for the last 1-μs simulations.

3 | RESULTS

3.1 | Validation of the sugar force field

To validate the force field for sugar molecules, we have investigated the binding of a β-D-galactopyranosyl-1-thio-β-D-galactopyranoside (TDG) molecule to a specific carbohydrate binding protein (PDB ID: 4JC1). This protein contains one binding site which is readily accessible by TDG from outside. Figure 3A shows the top view of the protein interacting with TDG at the binding site for simulations with both all-atom (left) and coarse-grained PACE (right) force fields. Some key residues (His158, Arg162, Asn174, and Glu184) interacting with TDG have been identified. As shown, the structure and orientation of the TDG with PACE are consistent with all-atom results with similar molecular interactions at the binding site. We also calculated the PMF by pulling the TDG out of the binding site. Directional harmonic constraints were applied on the TDG molecule[52] such that it has similar orientation to the protein binding site and can only move in the vertical direction. We choose the vertical distance from the center of the protein to the center of the TDG molecule as the reaction coordinate (z) (Figure 3B), and then perform the PMF calculations for both the CG and all-atom models using ABF method. As shown in Figure 3C, the PMF profile from CG model (green line) agrees well with the all-atom model (red line) around the binding site validating the sugar force field. There are some noticeable fluctuations for PMF from CG model as the TDG moves out of the binding site to the bulk water, which is due to the resolution transition from the protein (united-atom model) to water (MARTINI model).

3.2 | Sugar binding to LacY

From the X-ray crystal structures of LacY,[11–13] a hydrophilic binding pocket is located near the center of the protein. Based on extensive amount of experimental evidences,[2,7,11,53–57] several essential residues inside the binding pocket: Glu126 (helix IV), Arg144 (helix V), Trp151 (helix V), Glu269 (helix VIII), Arg302 (helix IX), His322 (helix X), and Glu325 (helix X), actively participate the substrate binding and play crucial roles on the overall lactose/H^+ symport process. With the new sugar force field, we first setup our simulations to investigate the binding process of a TDG molecule to a wild-type LacY (PDB ID: 2V8N). As illustrated in Figure 4A, a TDG molecule was initially placed near the binding pocket with the two sugar rings aligned vertical to the membrane and then allowed to relax to the binding pocket through appropriate salt-bridges and H-bonds interactions. We monitored the dynamics of TDG molecule through measuring the distance (d_{CM}) between the center of mass (CM) of TDG and the CM of several key residues (Arg144, Glu269, Asp237, and Lys358), and the angle (θ) formed by the line connecting the two rings of TDG ($C_4 - C_4^{'}$) to the horizontal direction as a function of simulation time. As shown in Figure 4B,C, the TDG molecule slowly translates to the binding pocket in 200 ns, concurrently the molecule adjusted itself through an orientational change from vertical to horizontal direction. The directional change may be caused by the stacking interactions between the Trp151 and the TDG ring as illustrated by the snapshot at the binding pocket in Figure 4D.[58] In addition, we also observed a strong salt-bridge formed by Arg144–TDG and weak salt-bridge by Lys358–TDG as indicated by the dashed lines. All the interactions are consistent with the captured X-ray structure of LacY with TDG substrate.[11] Moreover, to accommodate the TDG molecule, we also observed slight opening of the LacY at the cytoplasmic side compared with the original wild-type LacY without substrate (PDB ID: 2V8N).

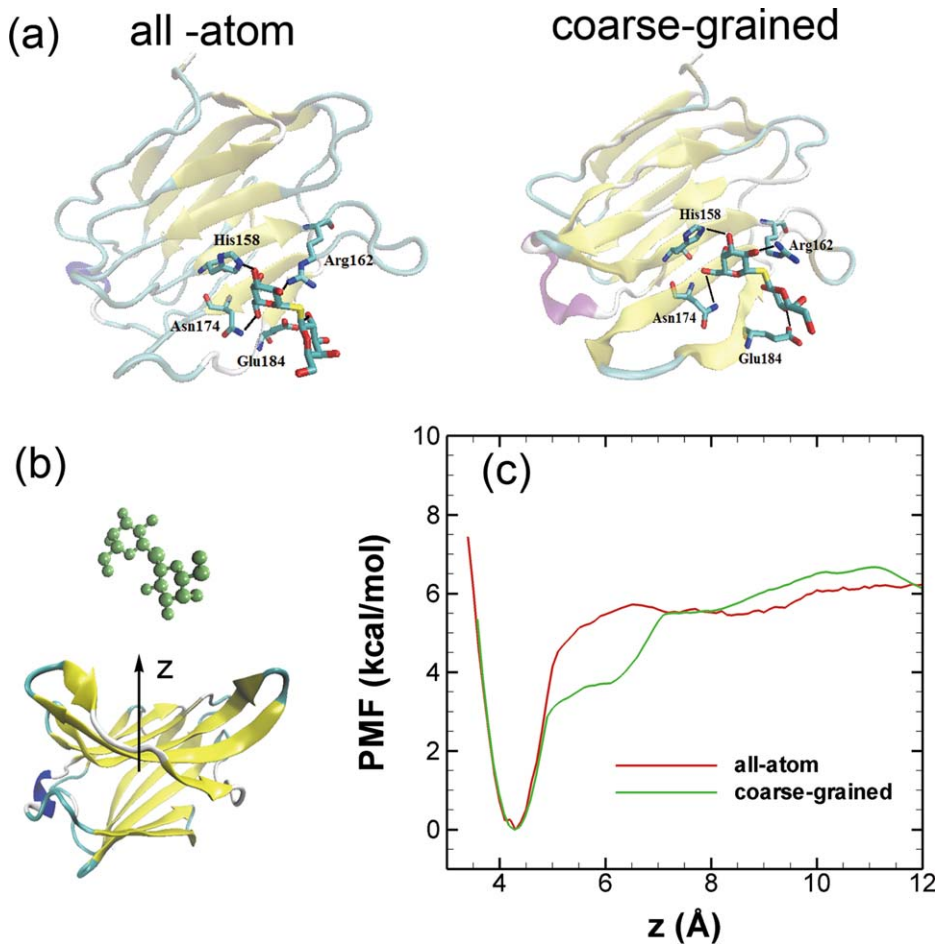

FIGURE 3 (a) Binding of a TDG molecule to a carbohydrate-binding protein (PDB ID: 4JC1) for all-atom (left) and coarse-grained (right) force field. (b) Simulation setup and definition of the reaction coordinate (*z*) for PMF calculations. (c) Comparison of PMFs between coarse-grained model (green) and all-atom model (red). [Color figure can be viewed at wileyonlinelibrary.com]

3.3 | LacY conformational changes and comparison with experiments

From a large amount of experiments and the mechanism illustrated in Figure 1, the proton translocation among Glu325, His322, and Glu269 plays crucial roles during the sugar transport and the associated LacY conformational changes. Protonation of Glu325 most likely stabilizes the inward-facing conformation, while the translocation of proton from Glu325 to Glu269 facilitates the LacY structural changes and triggers the transition from inward-facing to outward-facing conformations. We setup our simulations to investigate the conformational changes of LacY in response to sugar binding and proton translocation. A TDG molecule was placed at the binding pocket of wild-type LacY (PDB ID: 2V8N) with initial inward-facing configuration. In our simulations, two controls have been created with either Glu325 or Glu269 protonated, and in each case, three independent simulations were performed for statistical consistency. Implementation of the hybrid PACE force field enables us to explore the conformational changes in microseconds. From our simulation results, protonation of Glu325 does stabilize the inward-facing conformation as shown in Supporting Information, Figure S1. The interhelical distances measured for pairs V105–T310 at the periplasmic side (Supporting Information, Figure S1a) and N137–Q340 at the cytoplasmic side (Supporting Information, Figure S1b) are consistent with the values from crystal structure with inward-facing conformation for all three simulations. However, significant structural changes were observed when Glu325 was deprotonated and Glu269 protonated (as also illustrated by the movie in the Supporting Information). We have monitored the conformational changes through measurement of LacY lumen pore radius and compared with X-ray crystal structure. As shown in Figure 5, in crystal (initial) structure, the cytoplasmic side is open while the periplasmic side is tightly closed. From our simulations results with Glu269 protonated, all three simulations show a clear pore radius increase of ~4 Å from the crystal structure at the periplasmic side. At the cytoplasmic side, we observed a moderate pore radius decrease of ~1 Å in simulation 1 and a dramatic decrease of ~3.5 Å in simulations 2 and 3. In summary, simulations 2 and 3 yielded a clear outward-facing structure (illustrated in Figure 5A) with opening at the periplasmic side and complete closure at the cytoplasmic side. Simulation 1 ended with a structure with opening at the periplasmic side and partial closure at the cytoplasmic side. Although the cytoplasmic side is not tightly closed in simulations, the pore is narrow

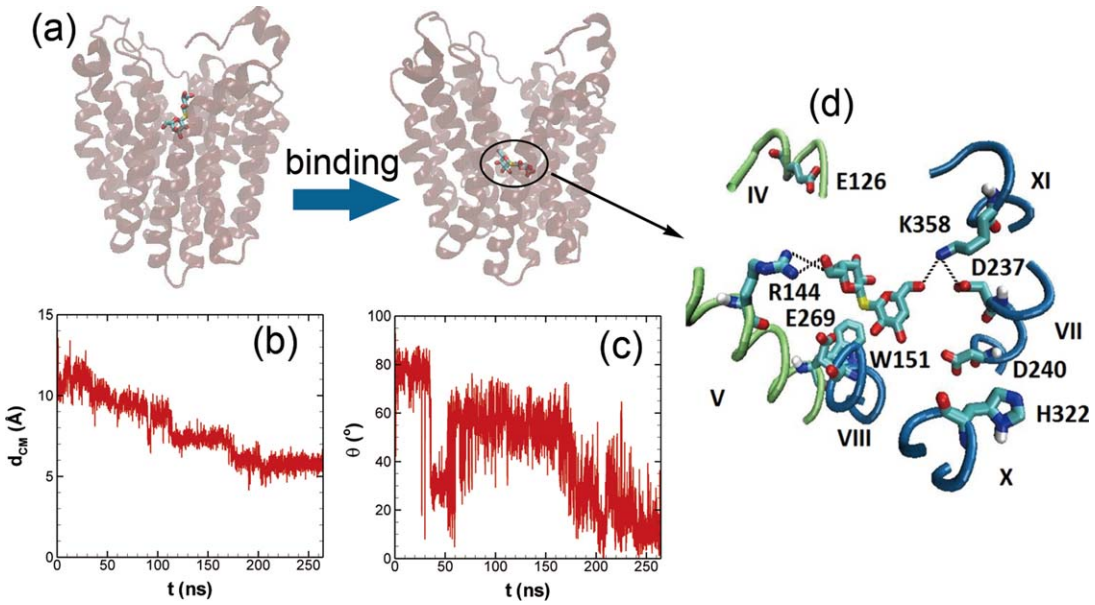

FIGURE 4 (a) The snapshots of LacY and TDG at initial stage before binding (left) and final stage after binding (right). The time evolution of (b) the distance between the center of mass of TDG and LacY binding pocket (d_{CM}) and (c) the angle formed by the line($C_4-C_4^{'}$) connecting TDG rings and horizontal direction (θ). (d) The substrate binding site of LacY. The key residues involved in TDG binding are labeled and the salt bridges are represented by black dashed lines. [Color figure can be viewed at wileyonlinelibrary.com]

enough to prevent the TDG moving out from the cytoplasmic side. Within our simulations, we did not observe any transport of TDG across LacY.

Smirnova et al.[17] have measured the interhelical distance changes using four-pulse DEER technique for a wild-type LacY during the conformational changes induced by sugar binding. In the experiments, nine nitroxide-labeled paired-Cys replacements were attached to both cytoplasmic and periplasmic end of LacY. Then the distance between each nitroxide-labeled pair was measured. From the measurements, the nitroxide-labeled pairs showed decreased distances ranging from 4 to 21 Å on the cytoplasmic side. On the periplasmic side, however, the nitroxide-labeled pairs exhibited increased distances ranging from 4 to 14 Å, clearly indicating a transition from inward-facing to outward-facing conformation. In our simulations, we measured the C_α–C_α difference in distance between exactly the same residue pairs relative to the X-ray crystal structure and compared with the DEER experiments in Figure 6. As shown, at the periplasmic side (pairs V105–T310, I164–T310, and I164–S375), all simulations showed significant increases by ~10–14 Å in pair distances. Our simulation results agree remarkably well with the experimental data. At the cytoplasmic side, the trend is consistent with the experiment showing decreased pair distances. The decreases in some pairs—such as R73–Q340, S136–Q340, and

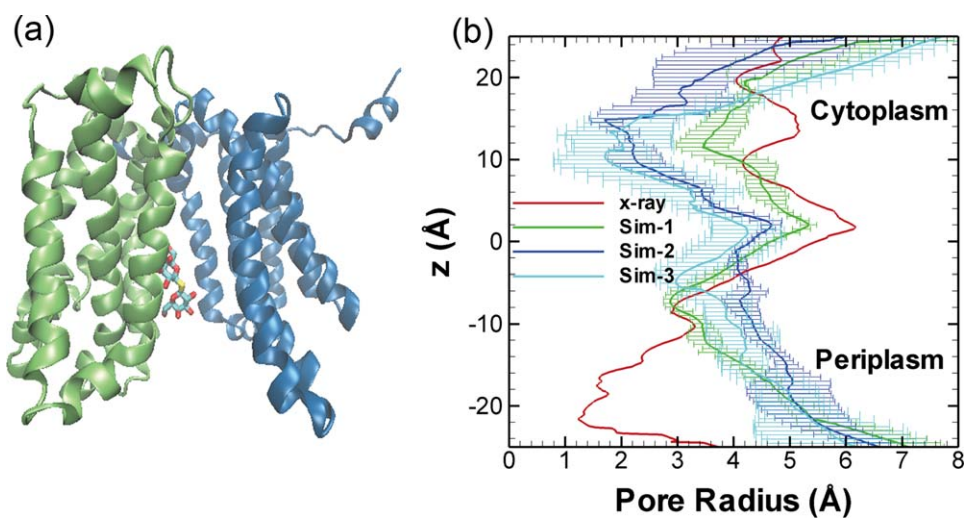

FIGURE 5 (a) The outward-facing LacY configuration at the end of the simulation 2. (b) The pore radius profiles of LacY. Simulations results (green: simulation 1; blue: simulation 2; cyan: simulation 3) are compared with the X-ray crystal structure (red). The error bars were calculated from 10 frames within the last 1 μs simulations. Simulations are for cases with Glu269 protonated

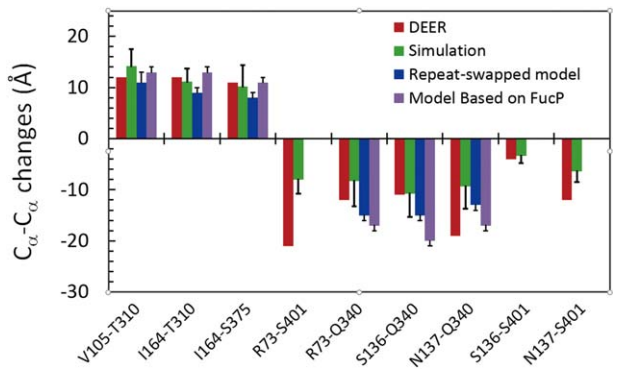

FIGURE 6 The $C_\alpha - C_\alpha$ difference in distance between residue pairs relative to the X-ray crystal structure. The first three pairs show increased distance indicating the opening of periplasmic side. The last six pairs show decreased distance indicating the closure of the cytoplasmic side. The data shown in red are from DEER experiment.[17] The data shown in blue and purple are from repeat-swapped model and model based on FucP.[30] The distances (green color) are the averaged values based on three independent simulations. [Color figure can be viewed at wileyonlinelibrary.com]

S136–S401 agreed well with the experiment, but the other pairs showed smaller decreases compared with the experimental data. In Refs. 29,31, the authors also explored the outward-facing state of LacY through a two-step hybrid implicit–explicit molecular simulation method. The outward-facing structure of LacY was generated with the aid of self-guided Langevin dynamics in an implicit membrane. Comparing our data with their results (Figure 8 in Ref. 29 and Figure 6 in Ref. 31), our results show slightly more opening at the periplasmic side and similar closure at the cytoplasmic side. Two outward-facing structural models of LacY have been generated through swapping the conformations of the repeat units in each half and through homology modeling with the structure of FucP as a template by Radestock and Forrest.[30] As shown in Figure 6, our simulations show similar opening at the periplasmic side and smaller closure at the cytoplasmic side comparing with the two models. However, as pointed out in Ref. 31, one should be careful in comparing with DEER data as the orientation and movement of the spin labels may significantly affect the residue pair distance measured in experiments. In general, the interhelical distance changes from our simulations indicate a transition from inward-facing to outward-facing conformation, which is consistent with the experiment and the pore radius measurement in Figure 5.

Moreover, Zhou et al.[23] have explored the opening/closing of the periplasmic side of LacY through cross-linking experiments. In the experiments, three paired double-Cys mutants (I40–N245, T45–N245, and I32–N245) located at the interface of the N- and C-terminal domains near the periplasmic end were constructed. Homobifunctional thiol cross-linking reagents of different lengths and flexibilities were used to test the influence of cross-linking on the transport activity of a TDG. It was found that the transport activity of sugar was almost completely blocked with cross-linking reagents of length less than ~15 Å. However, with the flexible reagents with length greater than ~15 Å, full or partial activity of sugar transport was observed. The experiments suggested that the opening of the periplasmic side was between 15 and 17 Å. Figure 7 shows the time evolution of the C_β–C_β distances between the three pairs: I40–N245, T45–N245, and I32–N245 throughout the simulations. Taking into account of the difference between the spacer arm distances in experiments and the C_β–C_β distances measured in our simulations, the experimental suggested opening of periplasmic side should be between 18.6 and 20.6 Å.[29] The experimental range has been indicated in Figure 7 as dashed lines for comparison. As shown, the C_β–C_β distances for all three pairs show consistent increase with time in all three simulations. In general, the steady-state C_β–C_β distances agree with the experimental data except some small differences, such as a slightly larger I40–N245 distance of ~22 Å in simulation 2 (Figure 7A) and slightly smaller T45–N245 distance of ~15 Å in simulation 1 (Figure 7B), were observed. Our results are also similar to the simulation data from Ref. 29 (Ex-r1 and Ex-r4 in Table 3).

3.4 | H-bonds/salt-bridges formation/breakage during LacY transition

All three simulations clearly indicate dramatic large-scale conformational changes from inward-facing to outward-facing upon the TDG binding and the protonation of Glu269. The structural changes are consistent with DEER[17], cross-linking[23] experiments, and modeling/simulations.[29–31] The overall global changes are the accumulative consequence of a complex and dynamical formation/breakage of salt-bridges and H-bonds among residues near the substrate binding site (Figure 4). Key residues and some important interactions playing crucial roles during lactose/H^+ symport have been identified by extensive site-directed and cysteine-scanning mutagenesis experiments,[2,59] and modeling/simulations.[25–28] As illustrated in Figure 1, fluorescence experiments[2,60] suggested that an interdomain H-bond between Trp151 (helix V) and Glu269 (helix VIII) should form and stabilize the inward-facing conformation of LacY. From our simulations as shown in Figure 8A, all simulations show significant increased distance between Trp151 and Glu269 indicating the breakage of the H-bond and opening of the periplasmic side. In addition, our simulations show a direct interaction and salt-bridge formation between Arg302 (helix IX) and Glu325 (helix X) within the C-terminal domain (Figure 8B) upon protonation of Glu269. This salt-bridge formation is consistent with the predictions from experiments[2,53] and repeated-swapped models[30] for outward-facing conformation of LacY. Moreover, we have also examined the interaction between Arg144 (helix V) and Glu269 (helix VIII) in all simulations. The X-ray structure suggested a direct salt-bridge interaction between Arg144 and Glu269 for inward-facing LacY with TDG.[11] However, our simulation results indicate a rather dynamic formation/breakage of salt-bridges with Glu325 protonated and no direct contacts with Glu269 protonated for Arg144–Glu269 interactions. This is probably due to the coarse-graining of the force filed or dynamic proton transfer among Glu269, His322, and Glu325, which is not considered in our current model. Finally, it is also interesting that in all simulations we observed the orientational movement of the TDG molecular from the horizontal to vertical direction with the conformational transition as

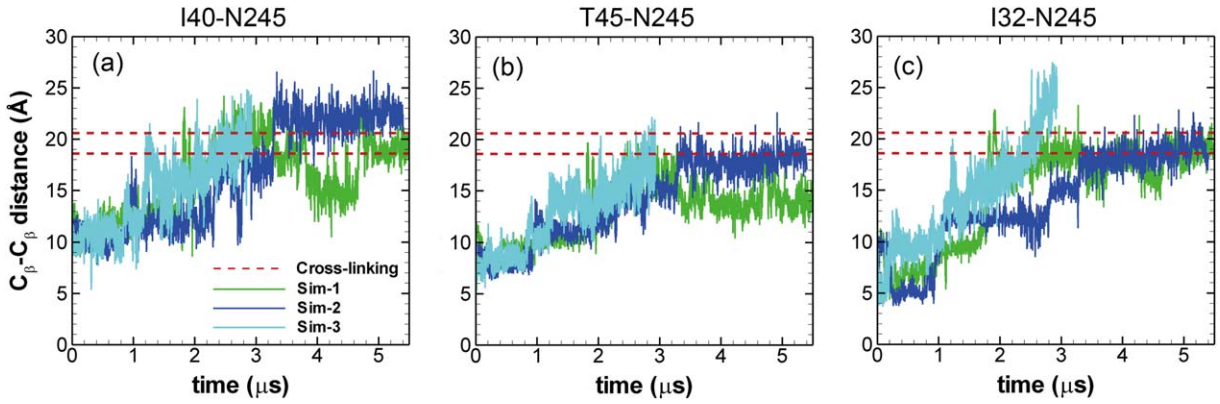

FIGURE 7 Time evolution of the $C_\beta - C_\beta$ distances between I40 and N245 (a), T45 and N245 (b), and I32 and N245 (c). The red dashed lines represent the value (18.6–20.6 Å) suggested from the cross-linking experiments for an outward-facing conformation.[23] Simulations are for cases with Glu269 protonated. [Color figure can be viewed at wileyonlinelibrary.com]

illustrated in Figure 5A. The partial/initial closure of the cytoplasmic side of LacY may be triggered by TDG reorientation.

4 | DISCUSSION AND CONCLUSIONS

The PACE force field, in which the united atom protein model is coupled with the MARTINI water/lipid models, has been extended to include interactions from sugar molecules. We have followed the same philosophy and procedures as the original PACE to parameterize both the bonded interactions within the sugar molecule and nonbonded sugar–water and sugar–protein interactions. The new force field was first validated by comparing the potential of mean force for TDG binding to a protein with the result from all-atom model. Then we implemented the force field to investigate the TDG binding to a wild-type inward-facing LacY and the protein conformational changes upon TDG binding and proton translocation. Simulation results showed that the molecular interactions (salt-bridges and H-bonds) between TDG and LacY at the binding pocket were consistent with the X-ray measurements of crystal structures. The implementation of the PACE force field has enabled us to explore the conformational changes of LacY in microsecond simulations (~5.5 μs). Our simulations demonstrated a clear transition from inward-facing to outward-facing conformation upon sugar binding and protonation of Glu269. The outward-facing configuration compared favorably with both DEER and cross-linking experiments, and previous modeling/simulations. Based on the analysis of the dynamics of H-bonds/salt-bridges and TDG molecule, a possible mechanistic picture of the LacY conformational transition emerges. First, protonation of the Glu269 disrupts the interdomain H-bonds, such as Trp151-Glu269, initiating the opening of the periplasmic side. Simultaneously, protonation of Glu269 also disturbs the TDG–LacY interactions and induces an orientational change of the TDG molecule from horizontal direction to vertical direction. Reorientation of the TDG molecule and the associated new TDG–LacY interactions may lead to further opening of the periplasmic side and partial closure of the cytoplasmic side of LacY. Finally, the formation of interdomain salt-bridges causes the complete closure of the cytoplasmic side. More systematic investigations are needed to obtain the molecular details involved in the sugar transport cycle and conformational changes of LacY. Nevertheless, as demonstrated in this work, the hybrid PACE force field is able to simultaneously achieve the computational efficiency and molecular details. It represents a powerful tool and holds great potential for investigation of lactose/H^+ symport across LacY.

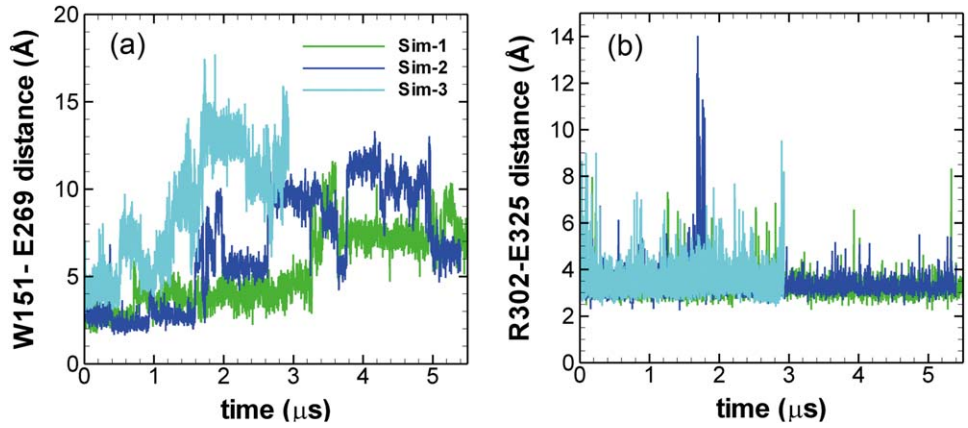

FIGURE 8 Time evolution of the interatomic (a) W151–E269 distance and (b) R302–E325 distance. The distance in (a) is measured between the indole N of Trp151 and the carboxyl group of Glu269. The distance in (b) is measured between the charged N of Arg322 and the carboxyl group of Glu325. Simulations are for cases with Glu269 protonated. [Color figure can be viewed at wileyonlinelibrary.com]

ACKNOWLEDGMENTS

This work was supported by US National Science Foundation under grant No. CBET-1604211. Computational resources were provided in part by the Extreme Science and Engineering Discovery Environment (XSEDE) under grant No. MCB170012.

REFERENCES

[1] Kaback HR. Structure and mechanism of the lactose permease. *C R Biol*. 2005;328(6):557–567.

[2] Guan L, Kaback HR. Lessons from lactose permease. *Annu Rev Biophys Biomol Struct*. 2006;35:67–91.

[3] Kaback HR. The lactose permease of Escherichia-coli - a paradigm for membrane-transport proteins. *Biochim Biophys Acta*. 1992;1101 (2):210–213.

[4] Sze T-kJ, Liu J, Dutta P. Numerical modeling of flow through phloem considering active loading. *J Fluids Eng*. 2014;136(2):021206.

[5] Sze T, kJ Liu J, Dutta P. Study of protein facilitated water and nutrient transport in plant phloem. *J Nanotechnol Eng Med*. 2014;4(3): 031005.

[6] Sze T-kJ, Liu J, Dutta P. Design and modeling of a light powered biomimicry micropump. *J Micromech Microeng*. 2015;25(6):065009.

[7] Mirza O, Guan L, Verner G, Iwata S, Kaback HR. Structural evidence for induced fit and a mechanism for sugar/H+ symport in LacY. *Embo J*. 2006;25(6):1177–1183.

[8] Guan L, Smirnova IN, Verner G, Nagamoni S, Kaback HR. Manipulating phospholipids for crystallization of a membrane transport protein. *Proc Natl Acad Sci USA*. 2006;103(6):1723–1726.

[9] Kwaw I, Sun JZ, Kaback HR. Thiol cross-linking of cytoplasmic loops in the lactose permease of *Escherichia coli*. *Biochemistry*. 2000;39 (11):3134–3140.

[10] Ermolova N, Guan L, Kaback HR. Intermolecular thiol cross-linking via loops in the lactose permease of *Escherichia coli*. *Proc Natl Acad Sci USA*. 2003;100(18):10187–10192.

[11] Abramson J, Smirnova I, Kasho V, Verner G, Kaback HR, Iwata S. Structure and mechanism of the lactose permease of *Escherichia coli*. *Science*. 2003;301(5633):610–615.

[12] Guan L, Mirza O, Verner G, Iwata S, Kaback HR. Structural determination of wild-type lactose permease. *Proc Natl Acad Sci USA*. 2007; 104(39):15294–15298.

[13] Chaptal V, Kwon S, Sawaya MR, Guan L, Kaback HR, Abramson J. Crystal structure of lactose permease in complex with an affinity inactivator yields unique insight into sugar recognition. *Proc Natl Acad Sci USA*. 2011;108(23):9361–9366.

[14] Smirnova I, Kasho V, Sugihara J, Kaback HR. Trp replacements for tightly interacting Gly-Gly pairs in LacY stabilize an outward-facing conformation. *Proc Natl Acad Sci USA*. 2013;110(22):8876–8881.

[15] Kumar H, Kasho V, Smirnova I, Finer-Moore JS, Kaback HR, Stroud RM. Structure of sugar-bound LacY. *Proc Natl Acad Sci USA*. 2014; 111(5):1784–1788.

[16] Jiang X, Smirnova I, Kasho V, et al. Crystal structure of a LacY–nanobody complex in a periplasmic-open conformation. *Proc Natl Acad Sci USA*. 2016;113(44):12420–12425.

[17] Smirnova I, Kasho V, Choe J-Y, Altenbach C, Hubbell WL, Kaback HR. Sugar binding induces an outward-facing conformation of LacY. *Proc Natl Acad Sci USA*. 2007;104(42):16504–16509.

[18] Majumdar DS, Smirnova I, Kasho V, et al. Single-molecule FRET reveals sugar-induced conformational dynamics in LacY. *Proc Natl Acad Sci USA*. 2007;104(31):12640–12645.

[19] Kaback HR, Dunten R, Frillingos S, et al. Site-directed alkylation and the alternating access model for LacY. *Proc Natl Acad Sci USA*. 2007;104(2):491–494.

[20] Nie Y, Ermolova N, Kaback HR. Site-directed alkylation of LacY: effect of the proton electrochemical gradient. *J Mol Biol*. 2007;374 (2):356–364.

[21] Nie YL, Kaback HR. Sugar binding induces the same global conformational change in purified LacY as in the native bacterial membrane. *Proc Natl Acad Sci USA*. 2010;107(21):9903–9908.

[22] Jiang XX, Nie YL, Kaback HR. Site-directed alkylation studies with LacY provide evidence for the alternating access model of transport. *Biochemistry*. 2011;50(10):1634–1640.

[23] Zhou YG, Guan L, Freites JA, Kaback HR. Opening and closing of the periplasmic gate in lactose permease. *Proc Natl Acad Sci USA*. 2008;105(10):3774–3778.

[24] Kaback HR, Smirnova I, Kasho V, Nie YL, Zhou YG. The alternating access transport mechanism in LacY. *J Membr Biol*. 2011;239(1–2): 85–93.

[25] Yin Y, Jensen MO, Tajkhorshid E, Schulten K. Sugar binding and protein conformational changes in lactose permease. *Biophys J*. 2006;91(11):3972–3985.

[26] Holyoake J, Sansom MSP. Conformational change in an MFS protein: MD simulations of LacY. *Structure*. 2007;15(7):873–884.

[27] Klauda JB, Brooks BR. Sugar binding in lactose permease: anomeric state of a disaccharide influences binding structure. *J Mol Biol*. 2007;367(5):1523–1534.

[28] Jensen MO, Yin Y, Tajkhorshid E, Schulten K. Sugar transport across lactose permease probed by steered molecular dynamics. *Biophys J*. 2007;93(1):92–102.

[29] Pendse PY, Brooks BR, Klauda JB. Probing the periplasmic-open state of lactose permease in response to sugar binding and proton trans location. *J Mol Biol*. 2010;404(3):506–521.

[30] Radestock S, Forrest LR. The alternating-access mechanism of MFS transporters arises from inverted-topology repeats. *J Mol Biol*. 2011; 407(5):698–715.

[31] Zhuang XH, Klauda JB. Modeling structural transitions from the periplasmic-open state of lactose permease and interpretations of spin label experiments. *BBA-Biomembranes*. 2016;1858(7):1541–1552.

[32] Han W, Wu Y-D. Coarse-grained protein model coupled with a coarse-grained water model: molecular dynamics study of polyalanine-based peptides. *J Chem Theory Comput*. 2007;3(6): 2146–2161.

[33] Han W, Wan C-K, Wu Y-D. Toward a coarse-grained protein model coupled with a coarse-grained solvent model: solvation free energies of amino acid side chains. *J Chem Theory Comput*. 2008;4(11): 1891–1901.

[34] Han W, Wan C-K, Jiang F, Wu Y-D. PACE force field for protein simulations. 1. Full parameterization of version 1 and verification. *J Chem Theory Comput*. 2010;6(11):3373–3389.

[35] Han W, Wan C-K, Wu Y-D. PACE force field for protein simulations. 2. Folding simulations of peptides. *J Chem Theory Comput*. 2010;6(11):3390–3402.

[36] Han W, Schulten K. Further optimization of a hybrid united-atom and coarse-grained force field for folding simulations: improved backbone hydration and interactions between charged side chains. *J Chem Theory Comput*. 2012;8(11):4413–4424.

[37] Wan C-K, Han W, Wu Y-D. Parameterization of PACE force field for membrane environment and simulation of helical peptides and helix-helix association. *J Chem Theory Comput*. 2012;8(1):300–313.

[38] Marrink SJ, de Vries AH, Mark AE. Coarse grained model for semiquantitative lipid simulations. *J Phys Chem B*. 2004;108(2):750–760.

[39] Marrink SJ, Risselada HJ, Yefimov S, Tieleman DP, de Vries AH. The MARTINI force field: coarse grained model for biomolecular simulations. *J Phys Chem B*. 2007;111(27):7812–7824.

[40] Jewel Y, Dutta P, Liu J. Coarse-grained simulations of proton-dependent conformational changes in lactose permease. *Proteins*. 2016;84:1067–1074.

[41] Kaminski GA, Friesner RA, Tirado-Rives J, Jorgensen WL. Evaluation and reparametrization of the OPLS-AA force field for proteins via comparison with accurate quantum chemical calculations on peptides. *J Phys Chem B*. 2001;105(28):6474–6487.

[42] Reith D, Putz M, Muller-Plathe F. Deriving effective mesoscale potentials from atomistic simulations. *J Comput Chem*. 2003;24(13):1624–1636.

[43] Zwanzig RW. High-temperature equation of state by a perturbation method. I. Nonpolar gases. *J Chem Phys*. 1954;22(8):1420–1426.

[44] Darve E, Rodriguez-Gomez D, Pohorille A. Adaptive biasing force method for scalar and vector free energy calculations. *J Chem Phys*. 2008;128(14).

[45] Phillips JC, Braun R, Wang W, et al. Scalable molecular dynamics with NAMD. *J Comput Chem*. 2005;26(16):1781–1802.

[46] Jo S, Kim T, Iyer VG, Im W. Software news and updates - CHARMM-GUI: a web-based graphical user interface for CHARMM. *J Comput Chem*. 2008;29(11):1859–1865.

[47] Jo S, Lim JB, Klauda JB, Im W. CHARMM-GUI membrane builder for mixed bilayers and its application to yeast membranes. *Biophys J*. 2009;97(1):50–58.

[48] Wu EL, Cheng X, Jo S, et al. CHARMM-GUI membrane builder toward realistic biological membrane simulations. *J Comput Chem*. 2014;35(27):1997–2004.

[49] Qi Y, Cheng X, Han W, Jo S, Schulten K, Im W. CHARMM-GUI PACE CG builder for solution, micelle, and bilayer coarse-grained simulations. *J Chem Inf Model*. 2014;54(3):1003–1009.

[50] Humphrey W, Dalke A, Schulten K. VMD: visual molecular dynamics. *J Mol Graph Model*. 1996;14(1):33–38.

[51] Smart OS, Goodfellow JM, Wallace BA. The pore dimensions of gramicidin-A. *Biophys J*. 1993;65(6):2455–2460.

[52] Woo HJ, Roux B. Calculation of absolute protein-ligand binding free energy from computer simulations. *Proc Natl Acad Sci USA*. 2005;102(19):6825–6830.

[53] Sahin-Toth M, Kaback HR. Arg-302 facilitates deprotonation of Glu-325 in the transport mechanism of the lactose permease from *Escherichia coli*. *Proc Natl Acad Sci USA*. 2001;98(11):6068–6073.

[54] He MM, Kaback HR. Interaction between residues Glu269 (helix VIII) and His322 (helix X) of the lactose permease of *Escherichia coli* is essential for substrate binding. *Biochemistry*. 1997;36(44):13688–13692.

[55] Sahin-Toth M, Karlin A, Kaback HR. Unraveling the mechanism of the lactose permease of *Escherichia coli*. *Proc Natl Acad Sci USA*. 2000;97(20):10729–10732.

[56] Frillingos S, Gonzalez A, Kaback HR. Cysteine-scanning mutagenesis of helix IV and the adjoining loops in the lactose permease of *Escherichia coli*: Glu126 and Arg144 are essential. *Biochemistry*. 1997;36(47):14284–14290.

[57] Smirnova I, Kasho V, Sugihara J, Choe J-Y, Kaback HR. Residues in the H+ translocation site define the pK(a) for sugar binding to LacY. *Biochemistry*. 2009;48(37):8852–8860.

[58] Guan L, Hu YL, Kaback HR. Aromatic stacking in the sugar binding site of the lactose permease. *Biochemistry*. 2003;42(6):1377–1382.

[59] Kaback HR, Sahin-Toth M, Weinglass AB. The kamikaze approach to membrane transport. *Nat Rev Mol Cell Biol*. 2001;2(8):610–620.

[60] Vazquez-Ibar JL, Guan L, Weinglass AB, Verner G, Gordillo R, Kaback HR. Sugar recognition by the lactose permease of *Escherichia coli*. *J Biol Chem*. 2004;279(47):49214–49221.

SUPPORTING INFORMATION

Additional Supporting Information may be found in the online version of this article.

How to cite this article: Jewel Y, Dutta P, Liu J. Exploration of conformational changes in lactose permease upon sugar binding and proton transfer through coarse-grained simulations. *Proteins*. 2017;85:1856–1865. https://doi.org/10.1002/prot.25340